Optica Applicata, Vol. XLIX, No. 1, 2019
DOI: 10.5277/oa190105

Ultrahigh nonlinear polarization maintaining dispersion compensating photonic crystal fiber

ASHISH KUMAR GHUNAWAT[1], RIM CHERIF[2], GHANSHYAM SINGH[1]

[1]Department of ECE, Malaviya National Institute of Technology, Jaipur, India

[2]Engineering School of Communication of Tunis, University of Carthage, Tunisia

[*]Corresponding author: akghunawat.ece@mnit.ac.in

This work describes the suitability of a nano-dimension slot with low index material in the core region to achieve a highly nonlinear, polarization maintaining and dispersion compensating photonic crystal fiber. Our design is composed of a spiral shaped photonic crystal fiber with an elliptical slot made of silicon nanocrystals in the core region. The simulated results show that high nonlinear coefficients at the 1.55 μm wavelength for quasi-TE mode and quasi-TM mode are found to be equal to 1348 and 638 $W^{-1}m^{-1}$, respectively. The proposed design offers high birefringence up to 0.2503 and large negative dispersion value –1228 ps/nm/km. The proposed fiber has immense potential for realization of all-optical signal processing devices/networks and sensing applications while maintaining its polarization.

Keywords: photonic crystal fiber, nonlinearity, birefringence, dispersion, nano-dimension slot, finite element method.

1. Introduction

Over preceding two decades, photonic crystal fibers (PCFs) have center-staged eminent significance due to their inherent remarkable properties and design flexibilities [1, 2]. PCFs have unique outstanding properties such as endlessly single mode operation [3], high nonlinearity [4–8], controlled dispersion [7, 8], high birefringence [9, 10], low confinement loss [10], *etc*. In recent years, advanced developments have been made in fiber structure. The structural developments in PCF have led to a new type of PCF with nano-scale slot in the core region. The term slot was coined by ALMEIDA *et al*. [11, 12] in reference to the slotted waveguides which is where it was first utilized to enhance the optical properties. The first expression of confining light in vertical slot-waveguides was performed on silicon nitride/silicon oxide material system [13]. This was followed by a study of group velocity dispersion of Si nanocrystal (Si-NC) filled horizontal slot waveguides. Around this time, it was established that Si-NC has a high nonlinear refractive index coefficient in the third optical window [14]. Due to the slot effect, the electric

field intensity gets further enhanced by a large factor. In 2014, a new structure spiral slotted PCF was proposed to obtain the nonlinearity coefficients of value 224 $W^{-1}m^{-1}$ (quasi -transverse-electric (TE) mode) and 226 $W^{-1}m^{-1}$ (quasi-transverse-magnetic (TM) mode) with very low dispersion [15]. Furthermore, Jianfei Liao *et al*. proposed a simple circle silicon microfiber design with a nano-dimensional low index slot inside to attain ultrahigh nonlinearity, large birefringence, with low dispersion values [16]. Tianye Huang *et al*. proposed another spiral PCF structure with an elliptical slot in the core region to get the benefit of a slot effect and nonlinearity values up to 1068 and 162 $W^{-1}m^{-1}$ and birefringence in the order of 10^{-1} was achieved [17].

Recently, highly nonlinear PCFs are getting much attention because of their extensive applications such as supercontinuum source generation [18–20], optical parametric amplification, all-optical wavelength conversion [21], distributed in-fiber amplification, pulse regeneration, optical monitoring, multiplexing and demultiplexing and switching [22]. In highly nonlinear PCF, power requirement of the optical device can be reduced [23] and the large nonlinearity can be achieved either by reducing the effective area of the core of PCF or using a material with a high nonlinear refractive index value [15, 16, 24–27]. To use effects of nonlinearity in photonic crystal fibers for applications, dispersion management is one of more pivotal concerns. Dispersion restricts the information carrying capacity of fiber so it is necessary to design dispersion compensation fiber to mitigate this effect. Besides nonlinearity and dispersion another important property of PCF is birefringence. PCF having high birefringence can be used as single-polarization mode fibers or polarization maintaining fibers (PMFs). Furthermore, birefringent PCFs have a very long list of important applications in optical sensor design, electro-optical modulation and signal processing systems [28, 29]. Recent works show that high birefringence in PCFs can be attained by introducing a defect in the core or generating asymmetricity in fiber structure [16, 17, 24, 26, 30]. As various nonlinear effects are polarization dependent, therefore sustaining the state of polarization is necessary for excellent performance.

To design an optical fiber having high nonlinearity, negative dispersion and large birefringence simultaneously is a continual challenge. Therefore, researchers are working on different geometries like hexagonal, octagonal, decagonal, spiral, *etc*. Our recent research study asserts that by using a slot spiral fiber design, negative dispersion, ultrahigh nonlinearity and high birefringence can be achieved. Currently, with the progress in fabrication techniques, silicon fibers which furnish a material compatibility with the traditional fiber structures, have gained a substantial attention. Due to its wide availability and compatibility with established CMOS technology, silicon offers reduction in structure sizes up to 10 nm at a very low cost [31, 32]. In this paper, slot spiral PCF structure is designed to achieve ultrahigh nonlinearity, high birefringence and large negative dispersion. Due to these properties, slot structures will have numerous applications in the optical field, *i.e*. biosensing [33]. For accurate analysis of optical characteristics of PCF, the finite element method (FEM) is applied.

2. Proposed structure of slot spiral PCF

The proposed slotted silicon PCF structure [15, 16] is shown in Fig. 1. All the circular air holes of the varying radius in the cladding are arranged in a spiral lattice. To obtain the good mode confinement in the core region, diameters of air holes in cladding region are in increasing order $d_1 < d_2 < d_3 < d_4$. The spiral lattice structure has six arms and each arm has four air holes. The radius of the first ring of circular holes is r. The air hole arranged in an arm is at an angular increment of $\theta = 30°$ with respect to the previous one. Position and angle of different air holes are:

- d_1: $x = r\cos(\pi/6)$, $y = r\sin(\pi/6)$;
- d_2: $x = 2r\cos(2\pi/6)$, $y = 2r\sin(2\pi/6)$;
- d_3: $x = 3r\cos(3\pi/6)$, $y = 3r\sin(3\pi/6)$;
- d_4: $x = 4r\cos(4\pi/6)$, $y = 4r\sin(4\pi/6)$;

where d_1 is the reference point, and order of increment is 30°. Value of θ for reference point $d_1 = 30°$.

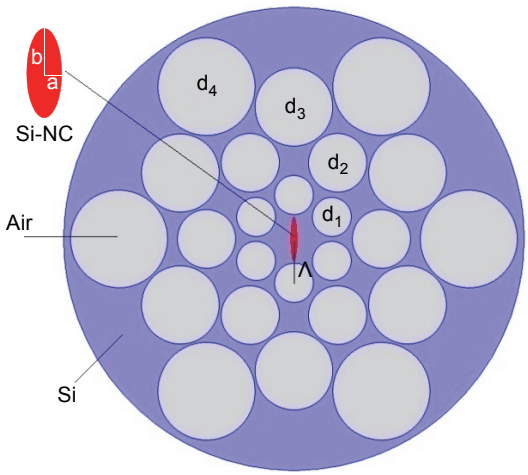

Fig. 1. Cross-sectional view of slotted spiral PCF.

The benefit of using the spiral lattice structure is that the number of air holes gets reduced compared to regular hexagonal or triangular lattice. This results in small effective mode area. To get the benefit of slot effect, an elliptical hole consisting of a material having a low index like Si-NC is embedded in the center of the core. At the interface of high index contrast, the electric field discontinuity is the primary principle of light confinement in nanometer size low index materials. The ratio of the refractive index of silicon to that of the slot material Si-NC enhances the electric field inside the slot region because the normal component of electric displacement ($D = \varepsilon E$) should be continuous across the interface [11]. Materials with high refractive index contrast at

the interface are preferred in order to boost the field enhancement in the low index slot region. The background of PCF is made of silicon which has a refractive index of 3.48 at 1.55 μm [34]. An elliptical slot is inserted in the core region having a semi-minor axis of *a* and semi-major axis of *b*. Refractive index of Si-NC can be calculated from the Sellmeier equation [14]

$$n^2(\lambda) = 1 + \frac{B_1\lambda^2}{\lambda^2 - C_1} + \frac{B_2\lambda^2}{\lambda^2 - C_2} + \frac{B_3\lambda^2}{\lambda^2 - C_3} \tag{1}$$

where $B_1 = 0.01$, $B_2 = 1.96$, $B_3 = 1.41$, $C_1 = 0.09$ μm^2, $C_2 = 0.005$ μm^2, $C_3 = 770.6$ μm^2 and λ is the wavelength of operation.

In comparison to a conventional fiber, the elliptical slot spiral PCF offers enhanced freedom in engineering nonlinearity, dispersion and birefringence. Nanometer size slot introduces asymmetry between the two axes and hence large birefringence is obtained. Due to the slot effect, light intensity gets enhanced leading to large nonlinearity. Our design consists of a slot core region surrounded by four rings of air holes in a spiral lattice whereas the design suggested in [15] has three rings of air holes in a spiral lattice. In our proposed design, air holes are enlarged in an ascending order to increase the index contrast which in turn improves the confinement whereas all air holes are of same size in the design considered in [15]. Hence, our proposed design gives us better results than the previously tried structure. Due to large variation in size of air holes, the proposed fiber structure shows large asymmetricity as compared to the design discussed in [15]. This large asymmetricity provides large birefringence compared to previous design. In [16] Jianfei Liao *et al*. have proposed a slotted microfiber without air holes in cladding which reduces the control over fiber properties like effective area, nonlinearity, birefringence, dispersion and confinement. While our proposed design consists of a slot core region surrounded by air holes which are enlarged in ascending order to increase the index contrast that results in better confinement. However, the proposed fiber provides reduced effective area that improves nonlinearity. Different size of air holes in the cladding region also generates asymmetricity in the fiber, which leads to high birefringence. Hence, the proposed design has better results than earlier proposed structures. Our design also displays high negative dispersion, which has been a limiting factor in the structures proposed earlier.

Due to rapid advancements in fabrication techniques [35–38], it is possible to fabricate silicon photonic crystal fibers with less hassle. Firstly, a silica PCF with an elliptical shaped air hole in the core of the fiber is fabricated. Then, silica PCF is converted to silicon microstructured fiber by using a magnesiothermic reduction technique. Finally, Si-NC layer is deposited in an elliptical air hole by applying the modified chemical vapour deposition (MCVD) method and then the proposed structure could be fabricated [39]. In the structure, the losses originating from multiple mechanisms can be classified into three groups – confinement loss, scattering loss and absorption loss. Scattering loss occurs due to imperfections in fiber surface which can be reduced by using upgraded fabrication techniques. The confinement loss of the design is low be-

cause the imaginary part of a quasi-TE mode is on the order of 10^{-7}. Confinement losses can be further reduced by employing more layers of air holes. It should be noted that the silicon fiber having losses nearby 5 dB/cm is feasible [40]. On that account, it is concluded that the proposed design can be used to realize all-optical signal processing.

3. Characterization and optical properties of slot spiral PCF

The finite element method (FEM) is used to determine the modal properties of the slot PCF structure. FEM has an automatic adaptive mesh refinement that is helpful in obtaining results with smaller error. The fiber design is simulated using COMSOL Multiphysics software. The cross-section of PCF is divided into small discrete elements; these allow us a better approximation of the PCF structure. Guided fundamental mode is the symmetric quasi-TE mode which has a high power confinement factor in the slot structure [41], the modal properties of another guided mode, quasi-TM mode, is also studied.

The field distribution of fundamental modes of the fiber at 1.55 μm is shown in Figs. 2**a** and 2**b** with optimum fiber parameters as Pitch(Λ) = 450 nm, a = 32 nm, b = 220 nm, d_1 = 400 nm, d_2 = 600 nm, d_3 = 800 nm, and d_4 = 1000 nm. The effective indexes of quasi-TM and quasi-TE modes are 2.7252 and 2.4749, respectively.

From Fig. 2**a** we can see that power confinement outside the slot region is very low for quasi-TE mode. The term vertical slot implies that at a vertical interface, electric field discontinuity takes place, meaning that the design supports quasi-TE polarization This electric field discontinuity is the main reason for the existence of a strong electric field inside the slot. When the slot is rotated in a horizontal direction, a quasi-TM mode will become the polarized mode.

3.1. Birefringence

The region to study the impact of slot geometry parameters on modal birefringence and the effects of slot width and height on the fiber birefringence is taken to be 1.495 to 1.825 μm. By using the FEM method to solve the Maxwell equation, we can obtain the optimum value of n_{eff}. Once we obtained the value of n_{eff}, birefringence B can be

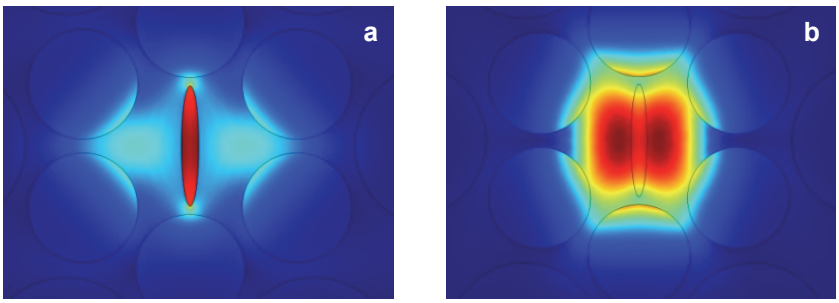

Fig. 2. Field distribution of fundamental modes. Quasi-TE mode (**a**) and quasi-TM mode (**b**) at 1.55 μm wavelength for vertically aligned Si-NC slot.

obtained by calculating the difference of effective indices of two fundamental modes as given by the following expression:

$$B = \left| n_{\text{eff}}^{x} - n_{\text{eff}}^{y} \right| \tag{2}$$

where n_{eff}^{x} and n_{eff}^{y} denote the refractive index of *x* polarization mode and *y* polarization mode, respectively. The ellipse-shaped slot significantly breaks the symmetry of PCF leading to a large variation in effective indices between the two fundamental modes. Progressively increasing the diameter of circular air holes in the cladding region not only provides a good mode confinement but it also disturbs the symmetry of the structure. Due to which very high birefringence is achieved.

In Figure 3**a**, birefringence increases as *a* increases. An increase in the slot width *a* leads to a higher confinement of light that will result in a large difference between fundamental modes. But this characteristic shows different behaviour for *b* values that are shown in Fig. 3**b**. Initially, birefringence values are increasing as the fiber parameter *b* increases for constant *a* = 32 nm, but after 220 nm the value of birefringence decreases. Because for small values of *a*, the maximum field is confined in the slot region but for higher values of *b* field enhancement weakens. This results in the reduction of effective refractive indices of two fundamental nodes. For optimum values of design parameters, the value of birefringence is obtained as 0.2503 at 1.55 μm wavelength.

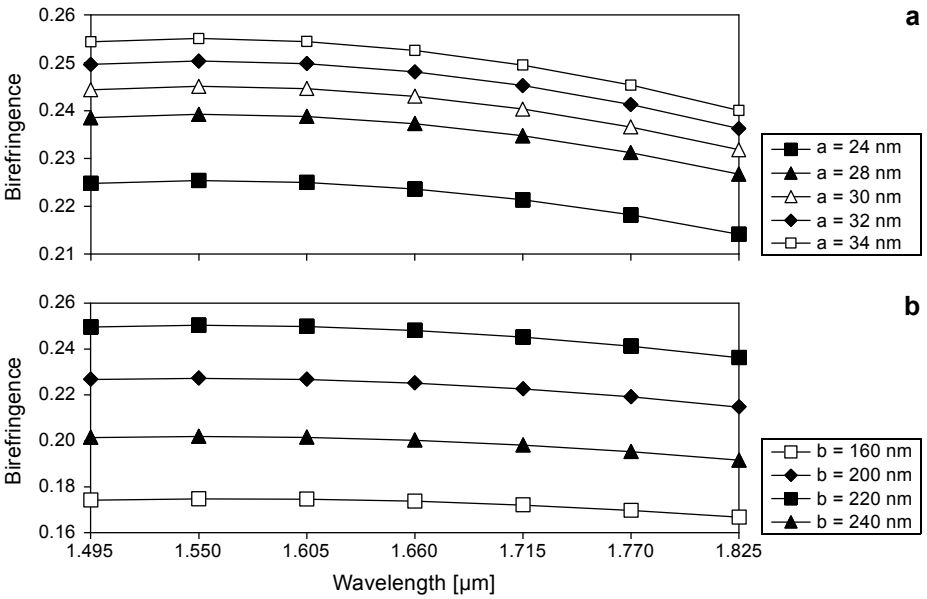

Fig. 3. Birefringence *vs*. wavelength for a vertical aligned slot in the core with variation in semi-minor axis *a* for *b* = 220 nm (**a**) and semi-major axis *b* for *a* = 32 nm (**b**).

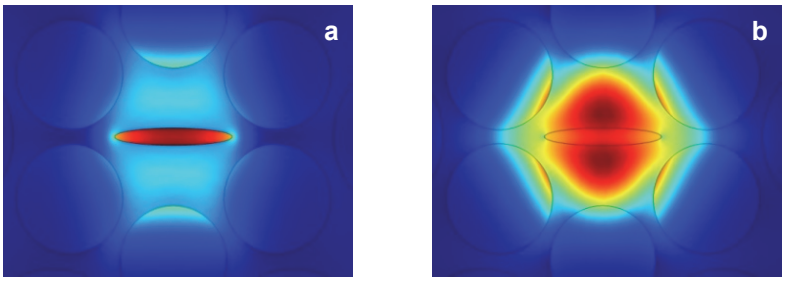

Fig. 4. Electric field intensity distribution of fundamental modes for quasi-TM mode (**a**) and quasi-TE mode (**b**) at 1.55 μm wavelength for a horizontally aligned slot.

If the slot is arranged in a horizontal direction, properties of the PCF design are changed slightly. At the following fiber parameters $\Lambda = 450$ nm, $a = 32$ nm, $b = 220$ nm, $d_1 = 400$ nm, $d_2 = 600$ nm, $d_3 = 800$ nm, and $d_4 = 1000$ nm, the electric field intensity distribution of fundamental modes is shown in Fig. 4.

The effective indexes of quasi-TM and quasi-TE modes are 2.4926 and 2.7179, respectively. For a horizontally aligned slot region, we have more flexibility to increase the dimensions of the slot. In this structure, due to a larger gap between two air holes along the vertical direction, the semi-major axis b can be varied for long length as compared to previous one.

Figure 5**a** depicts that as the values of a are increasing, more asymmetry is generated within the structure that will lead to higher birefringence. Similarly, for increasing

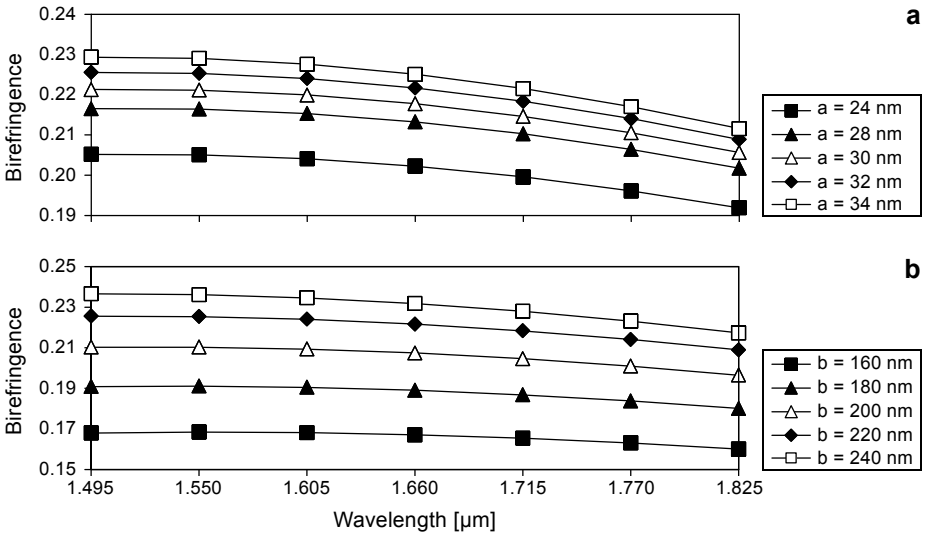

Fig. 5. Birefringence *vs*. wavelength for a horizontally aligned slot in the core with variation in semi-minor axis a for $b = 220$ nm (**a**) and semi-major axis b for $a = 32$ nm (**b**).

values of b, increased birefringence is also obtained as shown in Fig. 5**b**. For optimum values of design parameters, the obtained value of birefringence is 0.2253 at 1.55 μm wavelength. The polarization-holding capability of a birefringent fiber is known as beat length L_b, which is given by

$$L_b = \frac{2\pi}{\beta_x - \beta_y} = \frac{\lambda}{\Delta n_{\text{eff}}} \tag{3}$$

where β_x and β_y denote the propagation constant and Δn_{eff} denotes the effective indices difference of two modes which are orthogonal at wavelength λ; L_b denotes the light propagation length after which the two fundamental modes are in same polarization state. If birefringence is high then beat length will be small and have polarization maintaining capacity. Due to this reason, this design has the property of maintaining the SOP of the input wave.

3.2. Nonlinear coefficient

Another key property of photonic crystal fibers is nonlinearity. Nonlinear coefficient γ of proposed PCF can be obtained by using the following numerical equation [42]:

$$\gamma = \frac{2\pi n_2}{\lambda A_{\text{eff}}} \tag{4}$$

where n_2 denotes nonlinear refractive index of material, λ is wavelength of operation. Here, the nonlinear refractive indices of Si and Si-NC are 5×10^{-18} m^2/W [43] and 0.47×10^{-16} m^2/W, respectively [44]. Effective area of PCF (A_{eff}) is calculated by the following equation:

$$A_{\text{eff}} = \frac{\left(\iint_{-\infty}^{\infty} E^2 \,\mathrm{d}x\,\mathrm{d}y\right)^2}{\iint_{-\infty}^{\infty} E^4 \,\mathrm{d}x\,\mathrm{d}y} \tag{5}$$

The effective area of PCF depends on the electric field confinement in the core of the fiber. Small effective mode area results in large nonlinearity which would have many applications like parametric amplification, supercontinuum generation, soliton pulse transmission, four wave mixing (FWM) and many nonlinear applications [42].

In Figure 6, the nonlinear coefficient γ of PCF for both fundamental modes is shown with varying semi-minor axis a and semi-major axis b. It is evident from Fig. 6**a** that as we increase the value of a, the value of nonlinear coefficient decreases. The reason is that as we are increasing a, the effective mode area is increasing and hence the light confinement ability or confinement factor decreased. In Figure 6**b**, depicts the effect

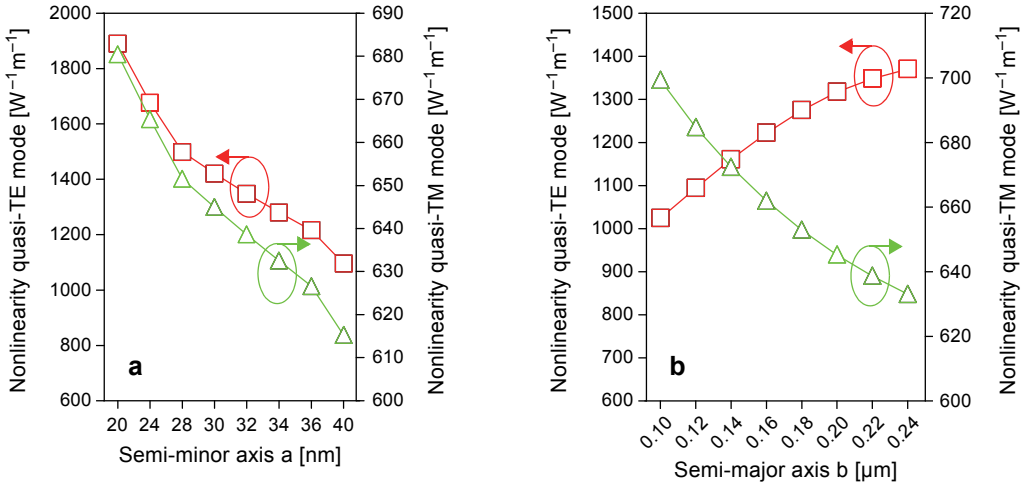

Fig. 6. Nonlinearity variation of the fundamental mode at 1.55 μm wavelength with variation in semi -minor axis *a* (**a**) and semi-major axis *b* (**b**).

of *b* on nonlinearity. As we increase *b*, nonlinearity increases as light becomes more confined. At 1.55 μm we have found that the nonlinear coefficient γ is 1348 and 638 $W^{-1}m^{-1}$ for quasi-TM and quasi-TE modes, respectively. In this proposed design, by varying the parameters, 1890 $W^{-1}m^{-1}$ is the highest achievable nonlinearity. For horizontal slot structure, the nonlinear coefficient γ for quasi-TE and quasi-TM modes are 1290 and 634 $W^{-1}m^{-1}$, respectively.

3.3. Chromatic dispersion

As dispersion limits the transmission distance and speed, it is necessary to compensate it for long haul transmission. For this purpose, we need to have a large negative dispersion for compensating the broadening of the pulse due to the inherited dispersion. Having large negative dispersion can also nullify the need of long fibers and help in reducing the cost. The summation of the material dispersion and the geometric dispersion is defined as the total chromatic dispersion. The wavelength dependence of the fiber material determines the material dispersion, the value of which cannot be changed after fabrication. On the other hand, the geometrical dispersion can be varied by altering the parameters of the fiber like pitch and hole size.

The total chromatic dispersion of the PCFs is calculated using given expression [42]:

$$D(\lambda) = -\frac{\lambda}{c}\frac{\partial^2 \mathrm{Re}(n_{\mathrm{eff}})}{\partial \lambda^2} \tag{6}$$

where *c* is the speed of light in vacuum and λ denotes the operating wavelength.

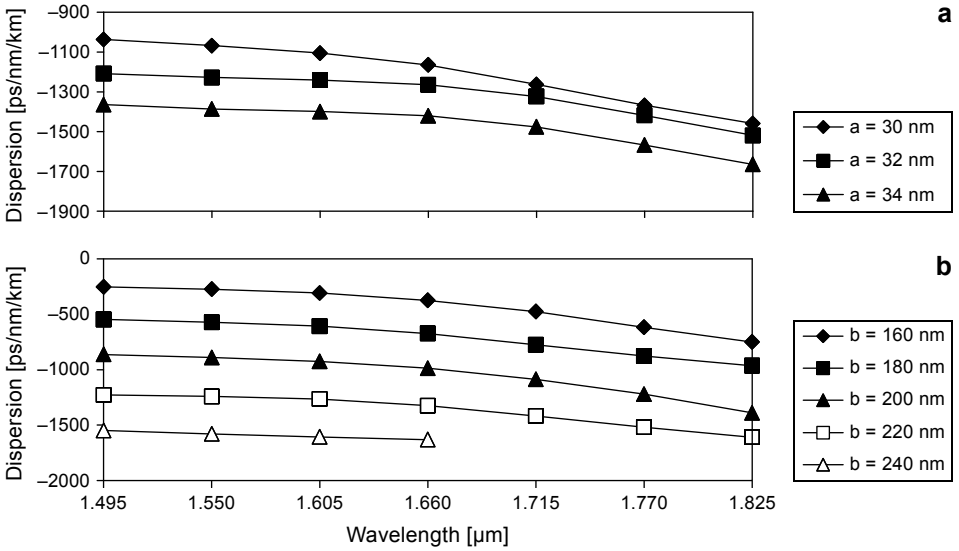

Fig. 7. Dispersion variation at 1.55 μm wavelength with semi-minor axis *a* (**a**), and semi-major axis *b* (**b**).

A strong light confinement region is created due to the large index contrast region between Si-NC and silicon. In this structure, dimensions of the slot region are at the nanometer scale. A small variation in any dimension of the slot region leads to large variation in total chromatic dispersion. Waveguide dispersion dominates the overall dispersion. In this particular region, the slot dimensions govern the total dispersion.

Figure 7 depicts the variation effect of semi-minor axis *a* and semi-major axis *b* on the chromatic dispersion of the proposed PCF design. One can notice from Fig. 7 that as values of *a* are increasing, dispersion values are decreasing rapidly. Similarly, for increasing values of *b*, dispersion values are decreasing sharply. So this large negative dispersion value makes this PCF design to be a good dispersion compensation element. At optimum parameters values at 1.55 μm wavelength, large negative dispersion value –1228 ps/nm/km is achieved. Whereas, in horizontally aligned slot structure for optimum design parameters, the dispersion of –1005 ps/nm/km is obtained at 1.55 μm.

4. Conclusion

By introducing a highly nonlinear elliptical slot in the core region, we are able to achieve ultrahigh nonlinearity and high birefringence with large negative dispersion. It has been shown through numerical results that by optimizing the fiber parameters, nonlinear coefficient of the fundamental mode, birefringence and dispersion at the wavelength of 1.55 μm are found to be equal to 1348 $W^{-1}m^{-1}$, 0.2503 and –1228 ps/nm/km, respectively. The proposed design can be used for nonlinear signal processing applications. This high birefringence can also be used in polarization maintaining fiber and many other applications such as sensing applications.

References

[1] Russell P., *Photonic Crystal Fibers*, Science **299**(5605), 2003, pp. 358–362, DOI: 10.1126/science.1079280.

[2] Ghunawat A.K., Jain A., Nikita K., Tiwari M., Singh G., *Optical Properties of Photonic Crystal Fibers*, [In] *Optical and Wireless Technologies*, [Eds.] Janyani V., Tiwari M., Singh G., Minzioni P., Lecture Notes in Electrical Engineering, Vol. 472, Springer, Singapore, 2018, pp. 265–275, DOI: 10.1007/978-981-10-7395-3_30.

[3] Birks T.A., Knight J.C., Russell P.St.J., *Endlessly single-mode photonic crystal fiber*, Optics Letters **22**(13), 1997, pp. 961–963, DOI: 10.1364/OL.22.000961.

[4] Lee J.H., Teh P.C., Yusoff Z., Ibsen M., Belardi W., Monro T.M., Richardson D.J., *A holey fiber based nonlinear thresholding device for optical CDMA receiver performance enhancement*, IEEE Photonics Technology Letters **14**(6), 2002, pp. 876–878, DOI: 10.1109/LPT.2002.1003123.

[5] Ghunawat A.K., Chandra R., Singh G., *Design of an ultra-flattened negative dispersion elliptical spiral photonic crystal fiber with high nonlinearity and high birefringence*, 2017 International Conference on Computer, Communications and Electronics (Comptelix), Jaipur, 2017, pp. 623–627, DOI: 10.1109/COMPTELIX.2017.8004044.

[6] Suryavanshi R.C., Ghunawat A.K., Jain S., Singh G., *Optimization of highly nonlinear soft glass photonic crystal fiber with high birefringence*, 2017 International Conference on Computer, Communications and Electronics (Comptelix), Jaipur, 2017, pp. 618–622, DOI: 10.1109/COMPTELIX.2017.8004043.

[7] Lu S., Li W., Guo H., Lu M., *Analysis of birefringent and dispersive properties of photonic crystal fibers*, Applied Optics **50**(30), 2011, pp. 5798–5802, DOI: 10.1364/AO.50.005798.

[8] Chengcheng Gui, Jian Wang, *Elliptical–spiral photonic crystal fibers with wideband high birefringence, large nonlinearity, and low dispersion*, IEEE Photonics Journal **4**(6), 2012, pp. 2152–2158, DOI: 10.1109/JPHOT.2012.2226149.

[9] Euser T., Schmidt M., Joly N., Gabriel C., Marquardt C., Zang L.Y., Förtsch M., Banzer P., Brenn A., Elser D., Scharrer M., Leuchs G., Russell P.St.J., *Birefringence and dispersion of cylindrically polarized modes in nanobore photonic crystal fiber*, Journal of the Optical Society of America B **28**(1), 2011, pp. 193–198, DOI: 10.1364/JOSAB.28.000193.

[10] Jianfei Liao, Junqiang Sun, *High birefringent rectangular-lattice photonic crystal fibers with low confinement loss employing different sizes of elliptical air holes in the cladding and the core*, Optical Fiber Technology **18**(6), 2012, pp. 457–461, DOI: 10.1016/j.yofte.2012.07.006.

[11] Almeida V.R., Qianfan Xu, Barrios C.A., Lipson M., *Guiding and confining light in void nanostructure*, Optics Letters **29**(11), 2004, pp. 1209–1211, DOI: 10.1364/OL.29.001209.

[12] Qianfan Xu, Almeida V.R., Panepucci R.R., Lipson M., *Experimental demonstration of guiding and confining light in nanometer-size low-refractive-index material*, Optics Letters **29**(14), 2004, pp. 1626–1628, DOI: 10.1364/OL.29.001626.

[13] Barrios C.A., Sánchez B., Gylfason K.B., Griol A., Sohlström H., Holgado M., Casquel R., *Demonstration of slot-waveguide structures on silicon nitride/silicon oxide platform*, Optics Express **15**(11), 2007, pp. 6846–6856, DOI: 10.1364/OE.15.006846.

[14] Spano R., Galan J.V., Sanchis P., Martinez A., Martí J., Pavesi L., *Group velocity dispersion in horizontal slot waveguides filled by Si nanocrystals*, 2008 5th IEEE International Conference on Group IV Photonics, 2008, pp. 314–316, DOI: 10.1109/GROUP4.2008.4638184.

[15] Jianfei Liao, Junqiang Sun, Mingdi Du, Yi Qin, *Highly nonlinear dispersion-flattened slotted spiral photonic crystal fibers*, IEEE Photonics Technology Letters **26**(4), 2014, pp. 380–383, DOI: 10.1109/LPT.2013.2293661.

[16] Jianfei Liao, Fan Yang, Yingmao Xie, Xinghua Wang, Tianye Huang, Zuzhou Xiong, Fangguang Kuang, *Ultrahigh birefringent nonlinear slot silicon microfiber with low dispersion*, IEEE Photonics Technology Letters **27**(17), 2015, pp. 1868–1871, DOI: 10.1109/LPT.2015.2443986.

[17] TIANYE HUANG, JIANFEI LIAO, SONGNIAN FU, TANG M., SHUM P., DEMING LIU, *Slot spiral silicon photonic crystal fiber with property of both high birefringence and high nonlinearity*, IEEE Photonics Journal **6**(3), 2014, article ID 2200807, DOI: 10.1109/JPHOT.2014.2323312.

[18] BAILI A., CHERIF R., HEIDT A., ZGHAL M., *Maximizing the bandwidth of coherent, mid-IR supercontinuum using highly nonlinear aperiodic nanofibers*, Journal of Modern Optics **61**(8), 2014, pp. 650–661, DOI: 10.1080/09500340.2014.905646.

[19] VYAS S., TANABE T., TIWARI M., SINGH G., *Chalcogenide photonic crystal fiber for ultraflat mid-infrared supercontinuum generation*, Chinese Optics Letters **14**(12), 2016, p. 123201.

[20] RIM CHERIF, AMINE BEN SALEM, MOURAD ZGHAL, BESNARD P., CHARTIER T., BRILLAND L., TROLES J., *Highly nonlinear As_2Se_3-based chalcogenide photonic crystal fiber for midinfrared supercontinuum generation*, Optical Engineering **49**(9), 2010, article ID 095002, DOI: 10.1117/1.3488042.

[21] YATSENKO YU.P., PRYAMIKOV A.D., *Parametric frequency conversion in photonic crystal fibers with germanosilicate core*, Journal of Optics A: Pure and Applied Optics **9**(7), 2007, pp. 716–722, DOI: 10.1088/1464-4258/9/7/025.

[22] TOULOUSE J., *Optical nonlinearities in fibers: review, recent examples, and systems applications*, Journal of Lightwave Technology **23**(11), 2005, pp. 3625–3641, DOI: 10.1109/JLT.2005.855877.

[23] WILLNER A.E., YILMAZ O.F., JIAN WANG, XIAOXIA WU, BOGONI A., LIN ZHANG, NUCCIO S.R., *Optically efficient nonlinear signal processing*, IEEE Journal of Selected Topics in Quantum Electronics **17**(2), 2011, pp. 320–332, DOI: 10.1109/JSTQE.2010.2055551.

[24] TIANYU YANG, ERLEI WANG, HAIMING JIANG, ZHIJIA HU, KANG XIE, *High birefringence photonic crystal fiber with high nonlinearity and low confinement loss*, Optics Express **23**(7), 2015, pp. 8329–8337, DOI: 10.1364/OE.23.008329.

[25] HAMEED M.F.O., OBAYYA S.S.A., EL-MIKATI H.A., *Highly nonlinear birefringent soft glass photonic crystal fiber with liquid crystal core*, IEEE Photonics Technology Letters **23**(20), 2011, pp. 1478–1480, DOI: 10.1109/LPT.2011.2163499.

[26] SAINI T.S., BAILI A., KUMAR A., CHERIF R., ZGHAL M., SINHA R.K., *Design and analysis of equiangular spiral photonic crystal fiber for mid-infrared supercontinuum generation*, Journal of Modern Optics **62**(19), 2015, pp. 1570–1576, DOI: 10.1080/09500340.2015.1051600.

[27] REVATHI S., INABATHINI S., SANDEEP R., *Soft glass spiral photonic crystal fiber for large nonlinearity and high birefringence*, Optica Applicata **45**(1), 2015, pp. 15–24, DOI: 10.5277/oa150102.

[28] SAITOH K., KOSHIBA M., *Single-polarization single-mode photonic crystal fibers*, IEEE Photonics Technology Letters **15**(10), 2003, pp. 1384–1386, DOI: 10.1109/LPT.2003.818215.

[29] JIAO S.L., TODOROVIĆ M., STOICA G., WANG L.V., *Fiber-based polarization-sensitive Mueller matrix optical coherence tomography with continuous source polarization modulation*, Applied Optics **44**(26), 2005, pp. 5463–5467, DOI: 10.1364/AO.44.005463.

[30] HAO RUI, *Highly birefringent photonic crystal fiber with a squeezed core and small modal area*, Optik **127**(13), 2016, pp. 5245–5248, DOI: 10.1016/j.ijleo.2016.03.045.

[31] VAN THOURHOUT D., VAN CAMPENHOUT J., ROJO-ROMEO P., REGRENY P., SEASSAL C., BINETTI P., LEIJTENS X.J.M., NOTZEL R., SMIT M.K., DI CIOCCIO L., LAGAHE C., FEDELI J.-M., BAETS R., *A photonic interconnect layer on CMOS*, 33rd European Conference and Exhibition of Optical Communication, 2007, Berlin, Germany, pp. 1–2, DOI: 10.1049/ic:2007022.

[32] TSYBESKOV L., LOCKWOOD D.J., ICHIKAWA M., *Silicon photonics: CMOS going optical*, Proceedings of the IEEE **97**(7), 2009, pp. 1161–1165.

[33] SAHU S., ALI J., SINGH G., *Optimization of a dual-slot waveguide for a refractive index biosensor*, Optica Applicata **48**(1), 2018, pp. 161–167, DOI: 10.5277/oa180115.

[34] BENTON C.J., *Solitons and nonlinear optics in silicon-on-insulator photonic wires*, Ph.D. Dissertation, Department of Physics, University of Bath, Bath, U.K., 2009.

[35] ADEMGIL H., HAXHA S., *Bending insensitive large mode area photonic crystal fiber*, Optik **122**(21), 2011, pp. 1950–1956, DOI: 10.1016/j.ijleo.2010.09.048.

[36] Vukovic N., Healy N., Peacock A.C., *Guiding properties of large mode area silicon microstructured fibers: a route to effective single mode operation*, Journal of the Optical Society of America B **28**(6), 2011, pp. 1529–1533, DOI: 10.1364/JOSAB.28.001529.

[37] Fatih Yaman, Hyungseok Pang, Xiaobo Xie, Patrick LiKamWa, Guifang Li, *Silicon photonic crystal fiber*, [In] *Conference on Lasers and Electro-Optics/International Quantum Electronics Conference*, OSA Technical Digest (CD), Optical Society of America, 2009, paper CTuDD7, DOI: 10.1364/CLEO.2009.CTuDD7.

[38] Belardi W., Bouwmans G., Provino L., Douay M., *Form-induced birefringence in elliptical hollow photonic crystal fiber with large mode area*, IEEE Journal of Quantum Electronics **41**(12), 2005, pp. 1558–1564, DOI: 10.1109/JQE.2005.858793.

[39] Songbae Moon, Aoxiang Lin, Bok Hyeon Kim, Watekar P.R., Won-Taek Han, *Linear and nonlinear optical properties of the optical fiber doped with silicon nano-particles*, Journal of Non-Crystalline Solids **354**(2–9), 2008, pp. 602–606, DOI: 10.1016/j.jnoncrysol.2007.07.088.

[40] Peacock A.C., Sparks J.R., Healy N., *Semiconductor optical fibers: progress and opportunities*, Laser and Photonics Reviews **8**(1), 2014, pp. 53–72, DOI: 10.1002/lpor.201300016.

[41] Zheng Zheng, Muddassir Iqbal, Jiansheng Liu, *Dispersion characteristics of SOI-based slot optical waveguides*, Optics Communications **281**(20), 2008, pp. 5151–5155, DOI: 10.1016/j.optcom.2008.07.003.

[42] Agrawal G.P., *Nonlinear Fiber Optics*, Academic Press, New York, 1995.

[43] Kai Jiang, Songnian Fu, Shum P., Chinlon Lin, *A wavelength-switchable passively harmonically mode-locked fiber laser with low pumping threshold using single-walled carbon nanotubes*, IEEE Photonics Technology Letters **22**(11), 2010, pp. 754–756, DOI: 10.1109/LPT.2010.2045647.

[44] Spano R., Daldosso N., Cazzanelli M., Ferraioli L., Tartara L., Yu J., Degiorgio V., Jordana E., Fedeli J.M., Pavesi L., *Bound electronic and free carrier nonlinearities in silicon nanocrystals at 1550 nm*, Optics Express **17**(5), 2009, pp. 3941–3950, DOI: 10.1364/OE.17.003941.

Received August 18, 2017
in revised form March 31, 2018